Enhancement of Chikungunya virus genome replication in mammalian cells at sub-physiological temperatures

Jinchao Guo[#] and Mark Harris*

School of Molecular and Cellular Biology, Faculty of Biological Sciences and Astbury Centre for Structural Molecular Biology, University of Leeds, Leeds, LS2 9JT, United Kingdom.

* Corresponding author, e-mail m.harris@leeds.ac.uk

[#] Current address: Department of Molecular Biology, Lewis Thomas Laboratory, Princeton University, Washington Road, Princeton, NJ, USA.

Word counts: Abstract: 249, Importance: 150, main text: 6718

9 Figures

Keywords: Chikungunya virus, alphavirus; subgenomic replicon; mammalian cells; sub-physiological temperature; stress granules

Short title: Chikungunya virus genome replication enhanced at sub-physiological temperatures

Author contributions: JG: conceptualization, formal analysis, investigation, visualization and writing. MH: conceptualization, funding acquisition, supervision, visualization and writing.

Abstract

Chikungunya virus (CHIKV) is an Alphavirus transmitted by *Aedes* mosquitoes, causing fever, rash and arthralgia. The function of the CHIKV non-structural protein 3 (nsP3) remains enigmatic. Building on previous studies (Gao *et al*, 2019), we generated a panel of mutants in a conserved and surface-exposed cluster in the nsP3 alphavirus unique domain (AUD) and tested their replication phenotype using a sub-genomic replicon (SGR) in mammalian and mosquito cells. Three mutants that replicated poorly in mammalian cells showed no defect in mosquito cells. These mutants were temperature-sensitive, rather than species-specific, as they exhibited no replication defect in mammalian cells at sub-physiological temperature (28°C). Similar effects were observed in the context of infectious CHIKV and the closely related O'Nyong Nyong virus. This analysis also revealed that the wildtype SGR replicated more efficiently at 28°C compared to 37°C. This was not due to either impaired interferon responses as the enhancement was observed in Vero cells, or to a defect in eIF2α phosphorylation as treatment with ISRIB, an inhibitor of global translation attenuation, did not compensate for replication defects at 37°C. The phenotype did correlate with enhanced recruitment of stress granule proteins (G3BP, eIF4G and TIA-1) into cytoplasmic sites of genome replication at 28°C. As cells in the periphery will be at sub-physiological temperatures, and will be the first cells infected in the mammalian host following a mosquito bite, we propose that alphaviruses such as CHIKV have evolved mechanisms to both promote viral genome replication and concomitantly limit antiviral responses in these cells.

Importance

Chikungunya virus (CHIKV) is a re-emerging arbovirus, transmitted by *Aedes* mosquitos and posing epidemic threats. Arboviruses must be able to replicate efficiently in both the mosquito vector and the mammalian host, at different temperatures. Following a mosquito bite the first cells infected will be in the skin and at sub-physiological temperature (less than 37ºC). We show that mutants in one of the CHIKV proteins (nsP3) could not replicate at 37ºC, but replicated efficiently in mammalian cells at 28°C. We also showed that wildtype CHIKV replicated more efficiently at 28°C in comparison to 37°C in mammalian cells. We investigated the mechanism behind this observation and showed that at sub-physiological temperatures proteins present in cytoplasmic stress granules were more efficiently recruited to sites of virus replication. We propose that CHIKV has evolved mechanisms to promote their replication in mammalian cells at sub-physiological temperatures to facilitate infection of mammals via a mosquito bite.

Introduction

Chikungunya virus (CHIKV) belongs to the *alphavirus* genus in the *Togaviridae* family [1]. It is an arbovirus that is transmitted by mosquitoes and causes fever, rash and arthralgia with infrequent long-term morbidity and in rare cases mortality [2]. CHIKV was first isolated in Tanzania in 1952-1953 [3, 4], and has subsequently spread across the world, including Africa, Europe, Asia and America [5, 6]. CHIKV is mainly transmitted by the mosquito species *Aedes aegypti* and *Ae. albopictus*, the latter has become the main vector for virus spread in Asia [7]. Both field and laboratory experiments demonstrated that the survival rate of these two mosquito species are affected by lower and upper temperature thresholds [8]. Models and human cases showed transmission occurs between 18°C and 34°C with maximal transmission occurring in a range from 26-29°C [9].

CHIKV has a positive-sense, single-stranded RNA genome, 11.5 kb in length, which is both capped and polyadenylated (Fig. 1A). It contains two open reading frames (ORFs), the first ORF encodes the non-structural proteins (nsP1-nsP4) and is translated directly from full-length genomic RNA. ORF2 encodes the structural proteins (Capsid, E1-E3 and 6K) and is translated from a sub-genomic RNA. The non-structural proteins are required for the synthesis of positive and negative full-length genomic RNA as well as the sub-genomic RNA. Biochemical analysis indicates specific functions of the non-structural proteins: nsP1 has methyl-and guanyl-transferase activities, nsP2 exhibits helicase and protease activities and nsP4 is the RNA-dependent RNA polymerase. The function of nsP3 remains poorly defined [10], although it is essential in genome replication. CHIKV nsP3 consists of three domains: a macro-domain at the N-terminus, a central alphavirus

unique domain (AUD) and a hypervariable domain (HVD) at the C-terminus (Fig 1A). The macro-domain exhibits RNA binding, ADP-ribose binding and ADP-ribosylhydrolase activities [11-13]. The HVD is highly phosphorylated and interacts with a number of host proteins [14]. Despite high levels of conservation across alphaviruses, AUD function remains elusive. In this context our recent work showed that the AUD binds to viral RNA and plays a role in virus assembly by stimulating transcription of the sub-genomic RNA and concomitant translation of ORF2 [15].

Eukaryotic initiation factor 2 (eIF2) is a key regulator of protein synthesis in mammalian cells [16]. Four eIF2 kinases (HRI, GCN2, PKR and PERK) phosphorylate the eIF2 α-subunit preventing guanine nucleotide exchange on eIF2 and resulting in global translational inhibition [17]. Although most alphaviruses possess an element within ORF2 that counteracts translational inhibition by phosphorylated eIF2α [18, 19], CHIKV does not contain this element and adopts an alternative strategy whereby CHIKV nsP4 has been shown to suppress eIF2α phosphorylation [20].

Translation inhibition via eIF2α phosphorylation results in the accumulation of stalled 48S mRNPs into cytoplasmic, non-membranous aggregates termed stress granules (SG). Typical SG contain silent mRNAs, translation factors, small ribosomal subunits, and various mRNA-binding proteins. Despite varied compositions resulting from different stresses [21], certain components including the RasGAP SH3-domain binding proteins (G3BP1/2), are required for formation of all SGs [22-24]. Alphavirus infection has been shown to block SG formation by sequestering critical proteins (such as G3BP1/2) into cytoplasmic foci which are the sites of genome replication [25, 26], as judged by the presence of both nsPs and double-stranded RNA in these foci. The CHIKV nsP3

hypervariable domain has been shown to interact with G3BP1/2 and recruit them to replication sites [27]. Recent work also demonstrated that the composition and disassembly of SG was determined by the ADP-ribosylhydrolase activity within the CHIKV nsP3 macro-domain [28].

In this study we sought to investigate the function of AUD in CHIKV replication in cells from both the vertebrate host and the mosquito vector. Three AUD mutants (W220A, D249A and Y324A) replicated poorly in mammalian cells but efficiently in mosquito cells, and we demonstrate that this phenotype was temperature-dependent rather than species-specific. Importantly, we also demonstrate that a wildtype CHIKV sub-genomic replicon (SGR) replicated more efficiently in mammalian cells at a sub-physiological temperature. Although phosphorylation of eIF2α was suppressed at lower temperature, it was not the key factor regulating the replication phenotypes observed. Subsequent analysis revealed that at the sub-physiological temperatures recruitment of critical SG proteins (G3BP, eIF4G and TIA-1) to cytoplasmic replication sites was enhanced. This provided a potential explanation for the enhanced genome replication at sub-physiological temperature.

Results

Construction and analysis of AUD mutants.

To identify conserved residues within the CHIKV AUD across the *Alphavirus* genus, a variety of AUD amino acid sequences from both Old and New World alphaviruses were aligned (Fig. S1A). The nsP2/nsP3 protein structure of Sindbis virus (SINV) has been determined [29], and the AUD sequences between SINV and CHIKV share high homology (118 out of 243 residues are identical). A panel of conserved and surface exposed residues in the AUD were therefore selected for mutation based on the SINV nsP2/nsP3 protein structure [29] (Figs. 1B and S1B). Seven residues were chosen for further study as they were either absolutely conserved or substituted by residues with similar physical characteristics. Y324 (nsP3 amino acid numbering) was selected as a control as it is located at the C-terminus of the AUD and conserved among alphaviruses. These mutations were introduced into a CHIKV dual luciferase sub-genomic replicon (CHIKV-SGR-D-Luc) (Fig. 1A), which was derived from the ECSA strain LR2006 OPY1 isolate [30, 31]. In this construct renilla luciferase (R-Luc) is fused within the nsP3 hypervariable domain in ORF1, and firefly luciferase (FF-Luc) replaces the structural proteins in ORF2. The activity of R-Luc is thus a marker of ORF1 translation from the full-length RNA: at early time points R-Luc levels reflect transfection efficiency and input RNA translation, at later times R-Luc is also dependent upon genome replication. As ORF2 is translated from a sub-genomic RNA (sgRNA) which is templated from the negative strand replicative intermediate, FF-Luc expression is dependent upon genome replication but will also reflect translation from the sgRNA. A polymerase-inactive mutant (GDD-GAA in nsP4) was used as a negative control.

AUD mutants exhibit different replication phenotypes in mammalian and mosquito cells.

CHIKV mainly induces arthritis and joint pain [2] and infects muscle cells. We therefore chose to investigate the effects of the AUD mutants on CHIKV genome replication initially in C2C12, an immortalized mouse myoblast cell line widely used in the study of CHIKV [32]. As expected, wildtype (WT) CHIKV-SGR-D-Luc showed a very high level of replication in C2C12 cells, with FF-Luc levels peaking at 12 h post transfection (h.p.t) and increasing over 1000-fold between 4-12 h.p.t. (Fig. 2A). AUD mutants T218Q, M219Q, P221A, C246A and A251Q exhibited similar levels of replication as compared to WT, however, W220A, D249A and Y324A showed significant lower levels of replication compared to WT (Fig. 2A). These results were paralleled by the R-luc levels, which also peaked at 12 h.p.t. with W220A, D249A and Y324A, showing significantly lower levels as compared to WT.

As CHIKV is transmitted by mosquitoes, we then evaluated the replication capacities of the AUD mutants in C6/36 and U4.4 cells, both derived from *Aedes albopictus*. Importantly, C6/36 cells harbor a frameshift mutation in the Dicer-2 (Dcr2) gene, which leads to the translation of a truncated Dcr2 protein and a defect in the RNAi response [33]. Consistent with this, although WT CHIKV-SGR-D-Luc showed robust replication in both cell lines, C6/36 supported higher levels of replication than U4.4 cells (Fig. 2B/C). Interestingly, unlike the replication defects observed in C2C12 cells, all AUD mutants showed similar levels of replication compared to WT in both C6/36 and U4.4 cells (Fig. 2B/C). In comparison to C2C12 cells, levels of both R-luc and FF-luc continued to increase up to 48 h.p.t.

The striking phenotypic differences between mammalian and mosquito cell lines for the three AUD mutants (W220A, D249A and Y324A) led us to investigate further. A simple explanation might be that these mutants had reverted to WT in mosquito cells, as we had previously observed this for the AUD mutant R243A/K245A [15]. This mutant replicated poorly in mammalian cells but efficiently in mosquito cells, and this was explained by the fact that R243A/K245A had reverted to WT in mosquito cells allowing efficient replication. To test this assumption, total RNA from U4.4 and C6/36 cells at 72 h.p.t was extracted, amplified by RT-PCR and sequenced. Surprisingly, none of the AUD mutants had reverted to WT, and all three mutants retained the same sequence as the input RNA (Fig. 2D). The results demonstrated that the ability of these three AUD mutants to replicate in mosquito cells was not due to reversion.

To confirm that the phenotype of the three AUD mutants was not specific to C2C12 cells we further investigated this in two other mammalian cells: RD (human rhabdomyosarcoma cells) and BHK-21 (baby hamster kidney fibroblasts). Reassuringly, all three AUD mutants showed replication defects compared to WT in both cell lines (Fig. 2E), although the magnitude of the defective phenotypes varied between the two cell lines. In particular the defective phenotypes were less apparent in BHK-21 cells, this is consistent with our observations of other mutants in nsP3 [34]. We conclude that the three residues W220, D249 and Y324 within the CHIKV nsP3 AUD play a role in genome replication in mammalian cells but not in mosquito cells.

The AUD mutants exhibit a temperature dependent phenotype.

We reasoned that a simple explanation for the different phenotypes in mammalian and mosquito cells might be the temperature difference, as mammalian cells are cultured at

37°C whereas mosquito cells are cultured at 28°C [35]. To test this, the replication of WT and mutant SGR-D-Luc were analysed in C2C12 cells incubated at 37°C or 28°C. Surprisingly, none of the three mutants exhibited any phenotype at the lower temperature, and both the FF-luc (Fig. 3A) and R-luc levels (Fig. S2A) were indistinguishable from WT at 28°C. In addition, although the absolute FF-luc levels in these experiments were lower than seen previously (Fig. 2A), most likely due to differences in the luminometer gain value to avoid saturating the detector , we noted that at 37°C WT CHIKV-SGR-D-Luc FF-luc levels plateaued at 12 h.p.t. In contrast, at 28°C FF-luc levels continued to increase (approximately 100-fold) from 12 to 24 h.p.t. As FF-luc levels were similar at both temperatures up to 12 h.p.t. this suggested that initial rates of replication and/or translation were temperature-independent, however after 12 h.p.t. these rates were limited at 37°C, but this limitation was relieved at the lower temperature. The optimal temperature for FF-Luc activity is between 22-28°C [36], so to confirm that this observation reflected a bona fide effect on genome replication and/or translation, rather than increased activity of the FF-Luc reporter at the lower temperature, translation of CHIKV SGR at the two temperatures was quantified by western blotting for nsP1 expression (Fig. 3B). Reassuringly, none of the mutants exhibited detectable nsP1 at 37°C whereas a low level of nsP1 was detectable for the WT at this temperature. In contrast, WT and all mutants exhibited high and equivalent levels of nsP1 at 28°C, consistent with the elevated levels of replication and translation at this temperature. To provide further support for the temperature difference we quantified both positive and negative strand CHIKV RNA over a period of 24 h.p.t. (Fig. 3C). Although the high level of input transfected RNA hampered quantification of genome replication at early time

points (eg 4 h.p.t.) a clear distinction in RNA levels could be seen at later time points. Specifically the levels of both positive and negative strand RNA declined at 37°C between 4-24 h.p.t. whereas at 28°C they continued to increase. By 24 h.p.t. there was at least a 10-fold higher level of CHIKV RNA at 28°C compared to 37°C.

We also observed the same enhanced replication at 28°C in Vero (African Green Monkey kidney epithelial) cells (Fig. S2B). These cells are IFN-deficient and thus unable to mount an IFN response following virus infection (although they possess IFN receptors and can respond to exogenous IFN). Our data therefore suggest that the enhanced replication at 28°C is not due to the previously documented reduced efficiency of the IFN response at sub-physiological temperatures [38]. We conclude that the three AUD mutants (W220A, D249A and Y324A) are temperature sensitive, exhibiting no defective phenotype in mammalian cells at a sub-physiological temperature. However, we also noted the novel observation that replication and/or translation of the WT CHIKV SGR was significantly enhanced at sub-physiological temperature.

To determine if this observation was unique to CHIKV or conserved within other alphaviruses we generated the same panel of mutants in the context of an infectious clone of the closely related virus, O'Nyong Nyong virus (ONNV). In this clone the fluorescent reporter ZsGreen was expressed from a sgRNA transcribed by a second copy of the sub-genomic promoter (ONNV-2SG-ZsGreen) (Fig. S3A) (kind gift from Prof. Andres Merits, University of Tartu). This construct enabled rapid assessment of genome replication by quantification of ZsGreen fluorescence per cell, as well as simultaneous measurement of infectious virus production by quantification of ZsGreen positive cells. Although expression of ZsGreen was dependent on genome replication as production of the sgRNA

is templated from the negative strand, the levels of ZsGreen expression are representative of both replication and translation of the sgRNA. As shown in Fig. S3B, the three AUD mutants (W220A, D249A and Y324A) showed a defect in replication at 37°C as judged by a reduction in the number of ZsGreen positive cells, whereas at 28°C the replication of all three was indistinguishable from WT. In addition, the absolute levels of ZsGreen per cell for WT was approximately 2-fold higher at 28°C compared to 37°C, consistent with enhanced genome replication at the sub-physiological temperature.

Enhanced replication at sub-physiological temperature is not dependent on the reporter protein, and is not exhibited by other arboviruses.

As the SGR-D-Luc construct contains two reporters, we considered it prudent to confirm that the phenotype we observed was not influenced by these reporters, or by the insertion of a reporter into nsP3. To test this, two alternative CHIKV SGRs were utilised, namely CHIKV-SGR-nsP3-mCh-FF-Luc (in which the R-Luc reporter was replaced with mCherry) and CHIKV-SGR-FF-Luc (lacking R-Luc and thus expressing WT unfused nsP3) (Fig. 4A). These two SGRs were assayed in parallel with CHIKV-SGR-D-luc in C2C12 cells at the two temperatures (28°C or 37°C). All three showed enhanced levels of replication at 28°C compared to 37°C (Fig. 4B). As described previously (Fig. 3A), this effect was most apparent between 12-24 h.p.t. These data confirm that enhanced genome replication at sub-physiological temperature is not dependent on the nature of the nsP3-fused reporter protein.

We reasoned that the enhancement of genome replication at sub-physiological temperature might be a common feature in other arboviruses that would share a mode of transmission from mosquitoes to humans via a peripheral bite. We therefore tested

replication of mini-genome constructs derived from Bunyamwera virus (BUNV), the type species of the genus Orthobunyavirus (negative-sense, single-stranded RNA viruses) [39] and an SGR derived from Zika virus, a positive-sense, single-stranded RNA virus in the *Flaviviridae* family [40]. As shown in Fig. 4C/D, although both the BUNV mini-genome [41] and the Zika nano-luc SGR [42] replicated poorly in BSR-T7 and BHK-21 cells respectively, they exhibited similar levels of genome replication at physiological and sub-physiological temperatures, indicating that this phenotype is not a common feature in other arboviruses.

Temperature sensitive AUD mutants retain the phenotype in the context of infectious CHIKV.

As we had previously identified a novel function of the CHIKV AUD in promoting virus assembly, we wished to determine whether the phenotypes we had observed in the context of CHIKV SGR were also seen in the context of infectious virus. The three AUD mutations (W220A, D249A and Y324A) were therefore generated in the ICRES-CHIKV infectious clone [31]. *In vitro* transcribed RNA for each construct was transfected into C2C12 cells and released virus was harvested at 48 h post infection (h.p.i) and titrated by plaque assay on BHK-21 cells. As shown in Fig. 5A, the three mutants produced significantly less infectious virus than WT at 37°C (approx. 10^4 reduction in titre). At 28°C, unlike the SGR data where the mutants were indistinguishable from WT, the mutants exhibited significantly reduced titres although this phenotype was much less pronounced than at 37°C (between 5-60 fold reduction). Sequence analysis of ICRES-CHIKV AUD mutants at 28°C or 37°C indicated that no reversion had occurred at either temperature (data not shown). Unlike the marked differences in genome replication observed using

SGRs, there was only a modest (albeit significant) increase (3-fold) in virus production at 28°C compared to 37°C. This suggested that the higher level of genome replication at 28°C did not lead to a concomitant increase in assembly and release of infectious virus, however, we noted that this result was obtained following transfection of *in vitro* transcribed RNA. We therefore performed a one-step growth curve analysis, evaluating virus production and genome replication over a time-course of 96 h following infection of C2C12 cells at a low MOI. As shown in Fig. 5B, the production of infectious virus was delayed at 28°C compared to 37°C, however the maximal titre reached was 5-fold higher (1.8×10^8 at 72 h.p.i. compared to 3.6×10^7 at 24 h.p.i.). A similar delay was observed when levels of intracellular positive and negative strand CHIKV RNA were quantified (Fig. 5C). Although there was no difference in the maximal levels of positive strand RNA, possibly due to higher level of packaging, assembly and release of infectious virus at the lower temperature (Fig. 5B), the level of negative strand RNA did attain a higher value. These data are consistent with the results obtained using SGR, namely that at later time points after infection the rate of genome replication was limited at 37°C but this limitation was relieved at the lower temperature. However, it should be noted that the differences observed in the context of infectious virus were not as marked as those seen in the SGR experiments, perhaps reflecting other cell factors or processes involved in assembly and release of infectious virus.

Temperature shift assay reveals that early events in SGR-D-Luc replication are not enhanced at sub-physiological temperature.

Previous studies have investigated temperature-sensitive mutants of alphaviruses by use of a temperature shift assay [43-45]. To further explore the role of temperature in

300 controlling CHIKV genome replication, a temperature shift assay was conducted in
301 C2C12 cells. WT CHIKV-SGR-D-Luc RNA was transfected into C2C12 cells and
302 incubated either at 37°C or 28°C for 12 h, with and without a subsequent temperature
303 shift from 12-24 h.p.t. (28°C to 37°C (designated S*), or 37°C to 28°C (designated S#))
304 (Fig. 6A). As seen previously (Fig. 3A), replication of WT SGR-D-Luc (as assessed by
305 FF-Luc levels) up to 12 h.p.t. proceeded at broadly similar rates at both temperatures (Fig.
306 6B), and between 12-24 h.p.t. replication increased ~100-fold at 28°C but did not increase
307 at 37°C. However, when the temperature was shifted from 28°C to 37°C at 12 h.p.t. (S*),
308 the replication increased only ~20-fold between 12-24 h.p.t. (Fig. 6B, left graph). The
309 opposite effect was seen when transfected cells were first incubated at 37°C: replication
310 reduced slightly between 12-24 h.p.t. at 37°C, however, when the temperature was
311 shifted from 37°C to 28°C at 12 h.p.t., replication increased 5-fold between 12-24 h.p.t.
312 (Fig. 6B, right graph).

313 Importantly, both cell growth assessed by quantification of viable cells (Fig. 6C), and
314 metabolic activity assessed by MTT assay (Fig. 6D) were higher at 37°C compared to
315 28°C. Temperature shifts elicited the expected changes in both cell number and
316 metabolic activity. These data confirmed that the enhanced replication observed at sub-
317 physiological temperature cannot be explained by increased cell growth and metabolic
318 activity. In fact, we observed an inverse correlation between virus genome replication
319 and cell growth and metabolic activity. These data were also confirmed by Western
320 blotting for nsP1 (Fig. 6E), demonstrating that translation of the 5' ORF was also
321 enhanced at the sub-physiological temperature. At this stage we also asked whether the
322 replication level was correlated with the level of phosphorylated eIF2α (P-eIF2α), given

that this is a critical factor in restricting translation during cell stress. However, there appeared to be little correlation between replication and levels of P-eIF2α (Fig. 6C), with the exception that when the temperature was shifted from 37°C to 28°C at 12 h.p.t. (S#), P-eIF2α levels reduced, coincident with an increase in replication (Fig. 6B, right hand graph).

A lack of involvement of eIF2α phosphorylation in the enhancement of genome replication at sub-physiological temperature was also demonstrated by experiments exploiting the small molecule ISRIB, shown to reverse the effects of eIF2α phosphorylation [46, 47]. As shown in Fig. S4A, FF-luc levels produced by the WT CHIKV-SGR-D-Luc were moderately stimulated by ISRIB treatment at both 28°C and 37°C, suggesting that eIF2α phosphorylation may make a minor contribution to regulating CHIKV genome replication and/or translation. However, although ISRIB treatment resulted in a modest increase in FF-luc levels for W220A CHIKV-SGR-D-Luc at 28°C, it was not able to restore replication of W220A at 37°C. The same outcome was observed in the context of infection with ONNV-2SG-ZsGreen (Fig. S4B). These data indicated that the temperature sensitive phenotype of W220A was not due to an inability to block eIF2α phosphorylation-mediated translational inhibition at 37°C.

Enhanced recruitment of stress granule proteins to replication sites at a sub-physiological temperature.

A well-described, if poorly understood, event during alphavirus infection is the sequestration of stress granule (SG) proteins such as the Ras-GAP SH3-domain-binding proteins (G3BP1/2) by nsP3. These proteins thus accumulate at cytoplasmic foci where viral genome replication occurs, leading to inhibition of the formation of bona fide SG [25,

26, 28, 48]. We considered that this function of nsP3 might play a role in the enhanced replication observed in mammalian cells at a sub-physiological temperature. SG formation can be induced by treatment with sodium arsenite ($NaAsO_2$) which results in oxidative stress, and they can be disassembled by cycloheximide (CHX) treatment. Importantly, it had been previously shown that $NaAsO_2$ was only able to induce SG at 37°C but not 28°C [49]. Using G3BP (detected using a pan-G3BP antibody) as a marker for the formation of bona fide SG we confirmed that this was also the case in our hands (Fig. S5), as no G3BP-positive SG were observed following $NaAsO_2$ treatment of C2C12 cells at 28°C. As expected, at 37°C SG were efficiently induced by $NaAsO_2$ treatment and disassembled by CHX.

To investigate this further we exploited the CHIKV SGR-nsP3-mCh-FF-luc construct in which nsP3 was fused to mCherry (see Fig. 4A), and we analysed the distribution and abundance of nsP3-mCherry and G3BP in transfected C2C12 cells (Fig. 7). As a further marker for sites of active genome replication (cytoplasmic foci) we also stained cells with an antibody to dsRNA (J2), previously shown by us [15] and others [26, 50] to co-localise with nsP1, nsP3 and G3BP. Consistent with previous data in this manuscript at 24 h.p.t. both dsRNA and nsP3-mCherry accumulated to a higher level at 28°C compared to 37°C, and this enhancement was not seen at earlier timepoints (Fig. 7B). In contrast, the amount of G3BP in infected cells increased over time and was higher at 37°C compared to 28°C.

We then quantified the co-localisation of nsP3, G3BP and dsRNA (Fig. 8). Plot line profiles revealed that all three colocalized at 28°C and 37°C when analysed at either 12 or 24 h.p.t. (Fig. 8A). Quantitative analysis (Fig. 8B) showed that at 12 h.p.t. there were

no differences in the amount of colocalized nsP3/G3BP, nsP3/dsRNA or G3BP/dsRNA, however at 24 h.p.t. the levels of colocalisation for all three pairs were significantly higher compared to 37°C. We confirmed these data by analysing the colocalisation of nsP3 and dsRNA with two other markers of SG which have been shown to be recruited to cytoplasmic replication sites: the eucaryotic translation initiation factor 4G (eIF4G) and T-cell intracytoplasmic antigen-1 (TIA-1), a granule-associated RNA-binding protein. Again, plot line profiles revealed that at 24 h.p.t. both eIF4G (Fig. 9A) and TIA-1 (Fig. 9B) colocalized with both nsP3 and dsRNA at 28°C and 37°C. Quantitative analysis again revealed that at 24 h.p.t., the co-localisation of eIF4G or TIA-1 with nsP3 and dsRNA was higher at 28°C compared to 37°C (Fig. 9C).

Taken together, these data are consistent with results shown in Fig 3 and confirm that at 28°C recruitment of SG proteins (G3BP, eIF4G and TIA-1) into sites of active genome replication (cytoplasmic foci) is more efficient than at 37°C. Concomitantly the number of active replication sites was higher at the non-physiological temperature.

Discussion.

This study started with the intention of building on our previous work which identified a role for two residues (P247 and V248) in the function of the CHIKV AUD [15]. Alanine substitution of these residues (termed the PV mutant) disrupted the binding of the AUD to the sub-genomic promoter, reducing transcription of the sub-genomic RNA and translation of structural proteins, with concomitant effects on virus assembly. In this study we generated a series of mutations in surface exposed and conserved residues proximal

to P247 and V248 to further investigate the phenotype. Surprisingly, most of these mutations had no effect on genome replication, although we cannot rule out an effect on virus assembly as this was not evaluated in this study. However, our experiments did demonstrate a role in genome replication for three residues W220, D249 and Y324, interestingly these residues are distal from each other (Fig. 1B). Indeed, Y324A was chosen as a control, being defined as the last residue in the AUD [29]. The phenotypes of the 3 mutants were observed in all mammalian cells tested although the magnitude of the defects varied somewhat. Intriguingly, in BHK-21 cells the mutants appeared to be better tolerated, as seen previously for both PV [15] and mutations in the nsP3 macrodomain [34]. Our study took a surprising turn when we observed that the 3 mutants exhibited no defective phenotype in mosquito cells and also when assayed in mammalian cells at sub-physiological temperatures, defining these as temperature-sensitive (ts) mutants. This analysis also revealed that the wildtype CHIKV replicated more efficiently at sub-physiological temperatures in mammalian cells and we focused our attentions on this intriguing observation. It should be noted that ts mutations in alphavirus nsP3 have been previously identified, for example in Sindbis virus F312S and A268V both resulted in a defect in negative-strand RNA synthesis at the non-permissive temperature (40°C) [51]. These data point to a critical role of nsP3, and the AUD in particular, in genome replication. Further biochemical analysis of these ts mutants in nsP3 may shed light on the specific role of nsP3.

It should be noted that, although enhancement of CHIKV genome replication at a sub-physiological temperature was observed in the context of CHIKV SGRs, it was not so apparent in the context of infectious virus. We observed only a modest increase in virus

production with delayed kinetics at sub-physiological temperatures, suggesting that other processes during the virus lifecycle (eg virus assembly and release) are also affected by temperature.

In considering why CHIKV genome replication in mammalian cells might be enhanced at sub-physiological temperatures, we reasoned that the first cells infected via a mosquito bite would be in the periphery and thus not at 37ºC. It would be reasonable to expect that other arboviruses would also exhibit the same differential, however, that was not the case as both BUNV and ZIKV replicated to similar levels at 28ºC and 37ºC. This suggests that this phenotype is driven by alphavirus specific processes, and we note that neither the nsP3 macrodomain nor the AUD have functional homologues in either bunyaviruses or flaviviruses. Analysis of the timescale of genome replication at different temperatures also revealed that the phenotype was most apparent after 12 h.p.t. In most cases, replication rates up to 12 h.p.t. did not differ between the two temperatures (eg see Fig. 3A), however between 12-24 h.p.t. replication continued to increase at 28ºC, but plateaued at 37ºC. One interpretation for this observation is that this reflects an aspect of the cellular response to virus genome replication that is perhaps ablated or blunted at the sub-physiological temperature. An obvious candidate would be the type 1 IFN response, which has indeed been shown to be reduced at lower temperatures promoting CHIKV arthritis in a mouse model [38]. However, our data suggest that this is not the explanation for our findings as we observed the same phenotype in Vero cells which are defective in IFN production.

An alternative possibility was that the host cell translational shutoff mediated by the phosphorylation of eIF2α was impaired at sub-physiological temperatures. However, we

437 were unable to determine any specific correlation between eIF2α phosphorylation and
438 genome replication (eg see Fig. 6E). In addition, treatment with ISRIB, a small molecule
439 that reverses the effects of eIF2α phosphorylation [47], failed to recapitulate the effect of
440 the lower temperature on replication of wildtype CHIKV or ONNV at 37ºC, and did not
441 permit the replication of W220A at 37ºC (Fig. S4). We therefore turned our attention to
442 stress granules (SG), cytoplasmic protein-mRNA aggregates formed in response to
443 stress and believed to play an antiviral role. Alphavirus infection has previously been
444 documented to disrupt formation of bona fide SG by recruiting key components of SG to
445 cytoplasmic foci where genome replication occurs [26], as judged by positivity for both
446 nsP3 and dsRNA. These include G3BP1/2, eIF4G and TIA-1, and, at least in the case of
447 G3BP1/2, these proteins have been shown to be critical for alphavirus genome replication
448 [23]. Sequestration of proteins such as G3BP1/2 away from bona fide SG will have the
449 added benefit of limiting the antiviral effects of SG.

450 Interestingly, as seen previously [49], treatment with $NaAsO_2$ (which induces oxidative
451 stress) did not result in SG formation at 28ºC (Fig. S5), suggesting that there was a defect
452 in this process at the sub-physiological temperature. However, following transfection with
453 a CHIKV SGR (expressing an mCherry-nsP3 fusion) we observed that SG components
454 (G3BP, eIF4G and TIA-1) were efficiently recruited into nsP3/dsRNA positive cytoplasmic
455 foci at both temperatures (Figs. 7-9). At 12 h.p.t. there was no difference in the co-
456 localisation of G3BP with nsP3 or dsRNA and in fact there were more nsP3/dsRNA
457 positive cytoplasmic foci at 37ºC (Fig. 7). However, at the later time point (24 h.p.t.) not
458 only were there more nsP3/dsRNA positive cytoplasmic foci at 28ºC (Fig. 7), but also the

recruitment of G3BP, eIF4G and TIA-1 to nsP3/dsRNA foci was significantly higher at 28ºC (Figs. 8, 9).

These data are consistent with the proposal that the enhanced level of CHIKV genome replication in mammalian cells at a sub-physiological temperature is associated with more efficient recruitment of cellular factors to cytoplasmic sites of replication. A likely explanation is that the absence of bona fide SG formation at 28ºC (Fig. S5), means that SG components are more abundant in the cytoplasm and this facilitates recruitment by nsP3 (or other nsPs). Further to this, our data suggest that the availability of SG components is not a limiting factor for genome replication until after 12 h.p.t. as there are no differences in replication or recruitment of SG factors to cytoplasmic foci at this timepoint at either temperature (see Figs. 3A, 8B).

Why the process of recruitment of SG components to cytoplasmic sites of replication should differ at different temperatures remains to be determined. However, importantly the ADP-ribosylhydrolase activity of the nsP3 macro-domain has recently been shown to play a key role in SG formation, disassembly and composition [28]. It is possible that the enzymatic activity and/or substrate specificity of the macrodomain could be modulated by temperature. Although the AUD *per se* has not been directly shown to play a role in SG formation, it is flanked by the macro-domain and HVD, both of which now have been implicated in SG formation. Localization of CHIKV nsP3 to cytoplasmic foci in invertebrate cells was shown to depend on both the AUD and the HVD [52], although it should also be noted that the interaction with G3BP1/2 (or its insect homologue, Rasputin) involves specific sequences within the HVD [53]. It is thus possible that all three domains

of nsP3 coordinate to control formation of bona fide SG, and recruit SG components to cytoplasmic sites of genome replication.

In conclusion, our data have revealed a hitherto unrecognized enhancement of CHIKV genome replication in mammalian cells at sub-physiological temperature that may play a role in the early stages of transmission of virus to the mammalian host via a mosquito bite. Our observations point to a critical role of the AUD in this difference, and our ongoing work seeks to understand the effects of temperature on the nsp3 interactions with host cell proteins using a proteomic approach.

Materials and methods.

Sequence alignment. AUD amino acid sequences in a variety of alphaviruses (Sindbis, Semliki, Ross River, Venezuelan, Eastern and Western Equine Encephalitis, ONNV and CHIKV) were obtained from NCBI and aligned by Clustal Omega. The conserved AUD residues were identified by Pymol and their locations were predicated from the Sindbis nsP2/3 protein structure (PDB ID code 4GUA) [15].

Cell culture. RD, Vero and BHK-21 cells were grown in DMEM supplied with 10% foetal calf serum (FCS), 0.5 mM non-essential amino acids and penicillin-streptomycin (100 units/mL). C2C12 cells were grown as above but with 20% FCS. All mammalian cells were maintained at 37°C or 28°C with 5% CO_2. RD cells were obtained from Nicola Stonehouse (University of Leeds), BHK-21 cells from John Barr (University of Leeds) and C2C12 cells from Michelle Peckham (University of Leeds). U4.4 and C6/36 cell lines (*Ae. albopictus*) were obtained from Susan Jacobs (The Pirbright Institute) and were cultured

503 in Leibovitz's L-15 media containing 10% FCS, 10% tryptose phosphate broth and
504 penicillin-streptomycin (100 units/mL), at 28°C without CO_2.

505 **Plasmid constructs.** CHIKV-SGR-D-Luc was used as a template for site-directed
506 mutagenesis using specific primers to generate each of the AUD mutations. The AUD
507 mutated fragments were excised and ligated back into the CHIKV-SGR-D-Luc backbone,
508 or into the infectious ICRES-CHIKV clone [31]. For construction of the ONNV AUD
509 mutants, a fragment including the AUD coding sequence was excised from the ONNV-
510 2SG-ZsGreen (donated by Prof. Andres Merits, University of Tartu), and ligated into
511 pcDNA3.1 to generate pcDNA3.1-ONNV-AUD. This was used as a template for site-
512 directed mutagenesis using specific primers to generate ONNV AUD mutations. The
513 ONNV AUD mutated fragments were excised from pcDNA3.1-ONNV-AUD and ligated
514 into the ONNV-2SG-ZsGreen backbone. CHIKV-SGR-nsP3-mCh-FF-Luc was generated
515 by SpeI digestion of the FF-Luc fragment from SGR-D-Luc and insertion of the mCherry
516 coding sequence. CHIKV-SGR-FF-Luc was constructed by SpeI digestion of the FF-Luc
517 fragment from SGR-D-Luc and self-ligation.

518 **Transfection and dual luciferase assay.** Capped RNAs of WT and mutant CHIKV-SGR-
519 D-Luc, ICRES-CHIKV, ONNV-2SG-ZsGreen, or WT CHIKV-SGR-nsP3-mCh-FF-Luc and
520 WT CHIKV-SGR-FF-Luc were synthesized and purified using the mMACHINE™ SP6
521 Transcription Kit (Thermo Fisher Scientific). In brief, 250 ng of each of the RNAs was
522 transfected into 5 x 10^4 cells using Lipofectamine 2000 (Life Technologies) according to
523 the manufacturer's instructions. Cells were harvested at 4, 12, 24 or 48 h.p.t. and both
524 FF-Luc and R-Luc activities were measured using the Dual-luciferase Kit (Promega)

525 according to the manufacturer's instructions. All experiments were repeated three times
526 independently.

527 **Sequence analysis.** Total RNA from transfected or infected cells was extracted with
528 Trizol, followed by reverse transcription to generate cDNA using the SuperScript IV
529 Reverse Transcriptase (Invitrogen) according to the manufacturer's instructions. The
530 expected DNA fragments of the CHIKV or ONNV genome were amplified by PCR using
531 specific primers (Primer sequences available upon request). Then all PCR products were
532 sequenced.

533 **MTT assay.** C2C12 cells were seeded into 96 well plates. The next day, cells were mock
534 transfected and incubated at 37°C or 28°C. At 4, 12 or 24 h.p.t, medium was removed
535 and replaced with 150 µl phenol-red free DMEM and 30 µl 6 mM MTT. Cells were
536 incubated at 37°C for 2 h before media was removed and replaced with 100 µl DMSO.
537 Plates were covered with foil and agitated until all MTT granules had dissolved, prior to
538 reading the absorbance at 570 nm.

539 **One-step growth curve of ICRES-CHIKV.** C2C12 cells were seeded into 12 well plates.
540 The next day, cells were infected with ICRES-CHIKV at MOI 0.1 and incubated at 37°C
541 for 1 h. The cells were then washed with PBS and replaced with fresh complete media,
542 followed by incubation at 37°C or 28°C respectively. Cell supernatants were harvested
543 at 0, 4, 8, 12, 24, 48, 72 and 96 h.p.i. for plaque assay, and cell monolayers were lysed
544 and extracted with TRIzol solution (ThermoFisher) for qRT-PCR analysis.

545 **Plaque assay.** Infected cell supernatants were harvested and stored at -80°C.
546 Supernatants were thawed, serially diluted and applied to monolayers of BHK-21 cells for

1 h at 37°C. The inocula were aspirated and cells were overlaid with 0.8% methylcellulose for 72 h at 37°C or 96 h at 28°C for ONNV infection, and 48 h at 37°C for ICRES-CHIKV. Plaques were either visualized by EVOS microscopy (ONNV) or staining with 0.05% crystal violet for 30 min (CHIKV).

qRT-PCR assay. C2C12 cell lysis containing transfected WT SGR-D-Luc RNA or ICRES-RNA were extracted by phenol-chloroform and total RNA were purified. Strand-specific CHIKV RNA primers were chosen from previous work [54] to amplify nucleotides 1-1560 of the CHIKV genome and used in reverse transcription reactions with the LunaScript8482 RT SuperMix Kit (NEB), followed by qPCR using the 2x qPCRBIO SyGreen Blue Mix (PCRBIOSYSTEMS). Positive and negative standards were generated using capped ICRES-CHIKV RNA with strand-specific RNA primers and were *in vitro* transcribed as described before.

Western blotting. Cells were lysed in passive lysis buffer (PLB) (Promega) or Glasgow Lysis Buffer (GLB) (10mM PIPES-NaOH pH7.2, 120mM KCl, 30mM NaCl, 5mM $MgCl_2$, 1% Triton X-100, 10% glycerol) supplemented with protease inhibitors and phosphatase inhibitors (Roche Diagnostics, specifically for detection of P-eIF2α), protein samples were quantified by BCA assay (Pierce). 10 or 20 µg of each sample was heat denatured at 95°C for 5 min and separated by SDS-PAGE, proteins were then transferred to polyvinylidene fluoride (PVDF) membrane and blocked with 50% (v/v) Odyssey blocking buffer (Li-Cor) diluted in 1X Tris-buffered saline Tween-20 (TBS-T) (50 mM Tris-HCl pH 7.4, 150 mM NaCl, 0.1% Tween-20). The membrane was then incubated with primary antibodies (1:1000 dilution) at 4°C overnight and the next day incubated with fluorescently labelled anti-mouse (700 nm) and anti-rabbit (800 nm) secondary antibodies for 1 h at

room temperature (RT). Membranes were then imaged on a Li-Cor Odyssey Sa Imager (Li-cor).

Immunofluorescence assay. C2C12 cells were seeded into 12 well plates with coverslips. The next day, cells were transfected with WT CHIKV-SGR-nsP3-mCh-FF-Luc as described before. At each time point (4, 12 or 24 h.p.t), cells were fixed with 4% formaldehyde,washed with PBS, permeabilized with ice-cold methanol at -20 °C for 10 min and blocked with 2% BSA for 1 h. The cells were incubated with primary antibody to G3BP (Abcam) (1:200), eIF4G (Thermo) (1:100 dilution) or TIA-1 (Thermo) (1:100 dilution) at 4°C overnight. The next day, cells were washed with DEPC-PBS and incubated with J2 dsRNA antibody (Scicons) (1:100 dilution) at RT for 1 h. All cells were stained with Alexa Fluor-594 chicken anti-rabbit and Alexa Fluor-647 goat anti-mouse secondary antibodies (1:500 dilution) at RT for 1 h. Cells were mounted onto glass slides with Prolong Gold antifade reagent (Invitrogen) containing 4',6'-diamidino-2-phenylindole dihydrochloride (DAPI) and sealed with nail varnish. Confocal microscopy images were acquired using a Zeiss LSM880 upright microscope. Post-acquisition analysis of images was performed using Zen software (Zen version 2018 black edition 2.3, Zeiss), or Fiji ImageJ (v1.49) software.

Statistical analysis. Statistical analysis was performed using the unpaired Student's t tests (two-tailed). Data in bar graphs represent statistically significant differences and displayed as the means ± S.E. of three experimental replicates (n = 3).

Acknowledgments

We thank Prof. Andres Merits (Institute of Technology, University of Tartu, Estonia) for the CHIKV SGRs, ICRES constructs, ONNV-2SG-ZsGreen construct and antibody to nsP1. We thank Dr. Andrew Tuplin for the Zika virus replicon and Dr John Barr for the BUNV mini-genome construct. We thank Drs. Niluka Goonawardane and Ruth Hughes for help in Fiji ImageJ analysis. We also thank Dr Sreenivasan Ponnambalam for access to the EVOS microscope.

Funding

This work was supported by a Wellcome Investigator Award to MH (grant number 096670). JG was supported by a University of Leeds/China Scholarship Council PhD studentship. The Zeiss LSM880 confocal microscope was funded by a Wellcome multi-user equipment grant (WT104818MA). The funders had no role in study design, data collection and analysis, decision to publish, or preparation of the manuscript.

References

[1] R. Chen, S. Mukhopadhyay, A. Merits, B. Bolling, F. Nasar, L.L. Coffey, A. Powers, S.C. Weaver, C. ICTV Virus Taxonomy Profile: Togaviridae, J Gen Virol 99(6) (2018) 761-762.

[2] O. Schwartz, M.L. Albert, Biology and pathogenesis of chikungunya virus, Nat Rev Microbiol 8(7) (2010) 491-500.

[3] M.C. Robinson, An epidemic of virus disease in Southern Province, Tanganyika Territory, in 1952-53. I. Clinical features, Trans R Soc Trop Med Hyg 49(1) (1955) 28-32.

[4] W.H. Lumsden, An epidemic of virus disease in Southern Province, Tanganyika Territory, in 1952-53. II. General description and epidemiology, Trans R Soc Trop Med Hyg 49(1) (1955) 33-57.

[5] I. Schuffenecker, I. Iteman, A. Michault, S. Murri, L. Frangeul, M.C. Vaney, R. Lavenir, N. Pardigon, J.M. Reynes, F. Pettinelli, L. Biscornet, L. Diancourt, S. Michel, S. Duquerroy, G. Guigon, M.P. Frenkiel, A.C. Brehin, N. Cubito, P. Despres, F. Kunst, F.A. Rey, H. Zeller, S. Brisse, Genome microevolution of chikungunya viruses causing the Indian Ocean outbreak, PLoS Med 3(7) (2006) e263.

[6] K. Sergon, C. Njuguna, R. Kalani, V. Ofula, C. Onyango, L.S. Konongoi, S. Bedno, H. Burke, A.M. Dumilla, J. Konde, M.K. Njenga, R. Sang, R.F. Breiman, Seroprevalence of Chikungunya virus (CHIKV) infection on Lamu Island, Kenya, October 2004, Am J Trop Med Hyg 78(2) (2008) 333-7.

[7] A.J. Tatem, S.I. Hay, D.J. Rogers, Global traffic and disease vector dispersal, Proc Natl Acad Sci U S A 103(16) (2006) 6242-7.

[8] O.J. Brady, M.A. Johansson, C.A. Guerra, S. Bhatt, N. Golding, D.M. Pigott, H. Delatte, M.G. Grech, P.T. Leisnham, R. Maciel-de-Freitas, L.M. Styer, D.L. Smith, T.W. Scott, P.W. Gething, S.I. Hay, Modelling adult Aedes aegypti and Aedes albopictus survival at different temperatures in laboratory and field settings, Parasit Vectors 6 (2013) 351.

[9] E.A. Mordecai, J.M. Cohen, M.V. Evans, P. Gudapati, L.R. Johnson, C.A. Lippi, K. Miazgowicz, C.C. Murdock, J.R. Rohr, S.J. Ryan, V. Savage, M.S. Shocket, A. Stewart Ibarra, M.B. Thomas, D.P. Weikel, Detecting the impact of temperature on transmission

of Zika, dengue, and chikungunya using mechanistic models, PLoS Negl Trop Dis 11(4) (2017) e0005568.

[10] J.C. Rupp, K.J. Sokoloski, N.N. Gebhart, R.W. Hardy, Alphavirus RNA synthesis and non-structural protein functions, J Gen Virol 96(9) (2015) 2483-2500.

[11] H. Malet, B. Coutard, S. Jamal, H. Dutartre, N. Papageorgiou, M. Neuvonen, T. Ahola, N. Forrester, E.A. Gould, D. Lafitte, F. Ferron, J. Lescar, A.E. Gorbalenya, X. de Lamballerie, B. Canard, The crystal structures of Chikungunya and Venezuelan equine encephalitis virus nsP3 macro domains define a conserved adenosine binding pocket, J Virol 83(13) (2009) 6534-45.

[12] L. Eckei, S. Krieg, M. Butepage, A. Lehmann, A. Gross, B. Lippok, A.R. Grimm, B.M. Kummerer, G. Rossetti, B. Luscher, P. Verheugd, The conserved macrodomains of the non-structural proteins of Chikungunya virus and other pathogenic positive strand RNA viruses function as mono-ADP-ribosylhydrolases, Sci Rep 7 (2017) 41746.

[13] R.L. McPherson, R. Abraham, E. Sreekumar, S.E. Ong, S.J. Cheng, V.K. Baxter, H.A. Kistemaker, D.V. Filippov, D.E. Griffin, A.K. Leung, ADP-ribosylhydrolase activity of Chikungunya virus macrodomain is critical for virus replication and virulence, Proc Natl Acad Sci U S A 114(7) (2017) 1666-1671.

[14] N.J. Foy, M. Akhrymuk, A.V. Shustov, E.I. Frolova, I. Frolov, Hypervariable domain of nonstructural protein nsP3 of Venezuelan equine encephalitis virus determines cell-specific mode of virus replication, J Virol 87(13) (2013) 7569-84.

[15] Y. Gao, N. Goonawardane, J. Ward, A. Tuplin, M. Harris, Multiple roles of the non-structural protein 3 (nsP3) alphavirus unique domain (AUD) during Chikungunya virus genome replication and transcription, PLoS Pathog 15(1) (2019) e1007239.

[16] T.E. Dever, Gene-specific regulation by general translation factors, Cell 108(4) (2002) 545-56.

[17] H.P. Harding, M. Calfon, F. Urano, I. Novoa, D. Ron, Transcriptional and translational control in the Mammalian unfolded protein response, Annu Rev Cell Dev Biol 18 (2002) 575-99.

[18] I. Ventoso, M.A. Sanz, S. Molina, J.J. Berlanga, L. Carrasco, M. Esteban, Translational resistance of late alphavirus mRNA to eIF2alpha phosphorylation: a strategy to overcome the antiviral effect of protein kinase PKR, Genes Dev 20(1) (2006) 87-100.

[19] R. Toribio, I. Diaz-Lopez, J. Boskovic, I. Ventoso, An RNA trapping mechanism in Alphavirus mRNA promotes ribosome stalling and translation initiation, Nucleic Acids Res 44(9) (2016) 4368-80.

[20] A.P. Rathore, M.L. Ng, S.G. Vasudevan, Differential unfolded protein response during Chikungunya and Sindbis virus infection: CHIKV nsP4 suppresses eIF2alpha phosphorylation, Virol J 10 (2013) 36.

[21] N. Kedersha, P. Anderson, Mammalian stress granules and processing bodies, Methods Enzymol 431 (2007) 61-81.

[22] N. Kedersha, M.D. Panas, C.A. Achorn, S. Lyons, S. Tisdale, T. Hickman, M. Thomas, J. Lieberman, G.M. McInerney, P. Ivanov, P. Anderson, G3BP-Caprin1-USP10 complexes mediate stress granule condensation and associate with 40S subunits, J Cell Biol 212(7) (2016) 845-60.

[23] H. Matsuki, M. Takahashi, M. Higuchi, G.N. Makokha, M. Oie, M. Fujii, Both G3BP1 and G3BP2 contribute to stress granule formation, Genes Cells 18(2) (2013) 135-46.

[24] H. Tourriere, K. Chebli, L. Zekri, B. Courselaud, J.M. Blanchard, E. Bertrand, J. Tazi, The RasGAP-associated endoribonuclease G3BP assembles stress granules, J Cell Biol 160(6) (2003) 823-31.

[25] M.D. Panas, T. Schulte, B. Thaa, T. Sandalova, N. Kedersha, A. Achour, G.M. McInerney, Viral and cellular proteins containing FGDF motifs bind G3BP to block stress granule formation, PLoS Pathog 11(2) (2015) e1004659.

[26] F.E. Scholte, A. Tas, I.C. Albulescu, E. Zusinaite, A. Merits, E.J. Snijder, M.J. van Hemert, Stress granule components G3BP1 and G3BP2 play a proviral role early in Chikungunya virus replication, J Virol 89(8) (2015) 4457-69.

[27] J.J. Fros, N.E. Domeradzka, J. Baggen, C. Geertsema, J. Flipse, J.M. Vlak, G.P. Pijlman, Chikungunya virus nsP3 blocks stress granule assembly by recruitment of G3BP into cytoplasmic foci, J Virol 86(19) (2012) 10873-9.

[28] A.K. Jayabalan, S. Adivarahan, A. Koppula, R. Abraham, M. Batish, D. Zenklusen, D.E. Griffin, A.K.L. Leung, Stress granule formation, disassembly, and composition are regulated by alphavirus ADP-ribosylhydrolase activity, Proc Natl Acad Sci U S A 118(6) (2021).

[29] G. Shin, S.A. Yost, M.T. Miller, E.J. Elrod, A. Grakoui, J. Marcotrigiano, Structural and functional insights into alphavirus polyprotein processing and pathogenesis, Proc Natl Acad Sci U S A 109(41) (2012) 16534-9.

[30] L. Pohjala, A. Utt, M. Varjak, A. Lulla, A. Merits, T. Ahola, P. Tammela, Inhibitors of alphavirus entry and replication identified with a stable Chikungunya replicon cell line and virus-based assays, PLoS One 6(12) (2011) e28923.

[31] K. Tsetsarkin, S. Higgs, C.E. McGee, X. De Lamballerie, R.N. Charrel, D.L. Vanlandingham, Infectious clones of Chikungunya virus (La Reunion isolate) for vector competence studies, Vector Borne Zoonotic Dis 6(4) (2006) 325-37.

[32] G.C. Roberts, C. Zothner, R. Remenyi, A. Merits, N.J. Stonehouse, M. Harris, Evaluation of a range of mammalian and mosquito cell lines for use in Chikungunya virus research, Sci Rep 7(1) (2017) 14641.

[33] E.M. Morazzani, M.R. Wiley, M.G. Murreddu, Z.N. Adelman, K.M. Myles, Production of virus-derived ping-pong-dependent piRNA-like small RNAs in the mosquito soma, PLoS Pathog 8(1) (2012) e1002470.

[34] G.C. Roberts, N.J. Stonehouse, M. Harris, The Chikungunya virus nsP3 macro domain inhibits activation of the NF-κB pathway, bioRxiv (2019).

[35] G.F. Zhu, Z.H. Liu, J. Wang, Improved technic for dengue virus micro cell culture, Chin Med J (Engl) 97(1) (1984) 73-4.

[36] M. Mehrabi, S. Hosseinkhani, S. Ghobadi, Stabilization of firefly luciferase against thermal stress by osmolytes, Int J Biol Macromol 43(2) (2008) 187-91.

[37] W.C. Lane, M.D. Dunn, C.L. Gardner, L.K.M. Lam, A.M. Watson, A.L. Hartman, K.D. Ryman, W.B. Klimstra, The Efficacy of the Interferon Alpha/Beta Response versus Arboviruses Is Temperature Dependent, mBio 9(2) (2018).

[38] N.A. Prow, B. Tang, J. Gardner, T.T. Le, A. Taylor, Y.S. Poo, E. Nakayama, T.D.C. Hirata, H.I. Nakaya, A. Slonchak, P. Mukhopadhyay, S. Mahalingam, W.A. Schroder, W. Klimstra, A. Suhrbier, Lower temperatures reduce type I interferon activity and promote alphaviral arthritis, PLoS Pathog 13(12) (2017) e1006788.

[39] V.H. Leonard, A. Kohl, T.J. Hart, R.M. Elliott, Interaction of Bunyamwera Orthobunyavirus NSs protein with mediator protein MED8: a mechanism for inhibiting the interferon response, J Virol 80(19) (2006) 9667-75.

[40] R.W. Malone, J. Homan, M.V. Callahan, J. Glasspool-Malone, L. Damodaran, B. Schneider Ade, R. Zimler, J. Talton, R.R. Cobb, I. Ruzic, J. Smith-Gagen, D. Janies, J. Wilson, G. Zika Response Working, Zika Virus: Medical Countermeasure Development Challenges, PLoS Negl Trop Dis 10(3) (2016) e0004530.

[41] F. Weber, E.F. Dunn, A. Bridgen, R.M. Elliott, The Bunyamwera virus nonstructural protein NSs inhibits viral RNA synthesis in a minireplicon system, Virology 281(1) (2001) 67-74.

[42] M. Mutso, S. Saul, K. Rausalu, O. Susova, E. Zusinaite, S. Mahalingam, A. Merits, Reverse genetic system, genetically stable reporter viruses and packaged subgenomic replicon based on a Brazilian Zika virus isolate, J Gen Virol 98(11) (2017) 2712-2724.

[43] J. Saraste, L. Kaaiainen, H. Soderlund, S. Keranen, RNA synthesis directed by a temperature-sensitive mutant of Semliki Forest virus, J Gen Virol 37(2) (1977) 399-406.

[44] L. Kaariainen, D. Sawicki, P.J. Gomatos, Cleavage defect in the non-structural polyprotein of Semliki Forest virus has two separate effects on virus RNA synthesis, J Gen Virol 39(3) (1978) 463-73.

[45] J. Suopanki, D.L. Sawicki, S.G. Sawicki, L. Kaariainen, Regulation of alphavirus 26S mRNA transcription by replicase component nsP2, J Gen Virol 79 (Pt 2) (1998) 309-19.

[46] C. Sidrauski, D. Acosta-Alvear, A. Khoutorsky, P. Vedantham, B.R. Hearn, H. Li, K. Gamache, C.M. Gallagher, K.K. Ang, C. Wilson, V. Okreglak, A. Ashkenazi, B. Hann, K.

Nader, M.R. Arkin, A.R. Renslo, N. Sonenberg, P. Walter, Pharmacological brake-release of mRNA translation enhances cognitive memory, Elife 2 (2013) e00498.

[47] C. Sidrauski, A.M. McGeachy, N.T. Ingolia, P. Walter, The small molecule ISRIB reverses the effects of eIF2alpha phosphorylation on translation and stress granule assembly, Elife 4 (2015) e05033

[48] M.D. Panas, M. Varjak, A. Lulla, K.E. Eng, A. Merits, G.B. Karlsson Hedestam, G.M. McInerney, Sequestration of G3BP coupled with efficient translation inhibits stress granules in Semliki Forest virus infection, Mol Biol Cell 23(24) (2012) 4701-12.

[49] J.R. Wheeler, T. Matheny, S. Jain, R. Abrisch, R. Parker, Distinct stages in stress granule assembly and disassembly, Elife 5 (2016) e18413

[50] D.Y. Kim, J.M. Reynaud, A. Rasalouskaya, I. Akhrymuk, J.A. Mobley, I. Frolov, E.I. Frolova, New World and Old World Alphaviruses Have Evolved to Exploit Different Components of Stress Granules, FXR and G3BP Proteins, for Assembly of Viral Replication Complexes, PLoS Pathog 12(8) (2016) e1005810.

[51] Y.S. Hahn, A. Grakoui, C.M. Rice, E.G. Strauss, J.H. Strauss, Mapping of RNA-temperature-sensitive mutants of Sindbis virus: complementation group F mutants have lesions in nsP4, J Virol 63(3) (1989) 1194-202.

[52] J.J. Fros, C. Geertsema, K. Zouache, J. Baggen, N. Domeradzka, D.M. van Leeuwen, J. Flipse, J.M. Vlak, A.B. Failloux, G.P. Pijlman, Mosquito Rasputin interacts with chikungunya virus nsP3 and determines the infection rate in Aedes albopictus, Parasit Vectors 8 (2015) 464.

[53] G. Nowee, J.W. Bakker, C. Geertsema, V.I.D. Ros, G.P. Goertz, J.J. Fros, G.P. Pijlman, A Tale of 20 Alphaviruses; Inter-species Diversity and Conserved Interactions

Between Viral Non-structural Protein 3 and Stress Granule Proteins, Front Cell Dev Biol 9 (2021) 625711.

[54] N.E. Plaskon, Z.N. Adelman, K.M. Myles, Accurate strand-specific quantification of viral RNA, PLoS One 4(10) (2009) e7468.

Figure legends

Figure 1. (**A**) **Structure of the CHIKV genome and nsP3.** The positive-sense RNA is capped and polyadenylated and templates translation of the 5′ORF into the four non-structural (ns) proteins which transcribe a negative-sense intermediate. Transcription of a sub-genomic RNA is then initiated from the sub-genomic promoter (sg-prom) and acts as a template for translation of the 3′ORF encoding the structural proteins. nsP3 comprises 3 domains: Macro-domain, AUD (alphavirus unique domain), HVD (hypervariable domain). The structure of the CHIKV dual luciferase sub-genomic replicon (CHIKV SGR-D-luc) is shown. R-Luc (Renilla luciferase) is expressed as a fusion within nsP3, FF-Luc (firefly luciferase) is expressed from the sg-prom. **(B) Three-dimensional structure of the SINV AUD [29].** Surface exposed and conserved residues targeted for mutagenesis are highlighted in the corresponding colours.

Figure 2. Replication of CHIKV AUD mutants in mammalian and mosquito cells. (**A**) C2C12, **(B)** C6/36, **(C)** U4.4, and **(E)** RD and BHK-21 cells were transfected with wildtype (WT) or mutant CHIKV-SGR-D-Luc and cells were harvested at indicated time points. FF-Luc activities of WT and mutants were measured and normalized to their respective 4 h values and thus represent fold-change compared to those 4 h values. (GAA: nsP4

polymerase inactive mutant). Significant differences denoted by ** (P<0.01), *** (P<0.001), **** (P<0.0001), compared to WT are only shown for the 12 h time point for clarity. Data are displayed as the means ±S.E. of three experimental replicates. (**D**) RT-PCR and sequence analysis of CHIKV-SGR-D-Luc W220A, D249A and Y324A in U4.4 and C6/36 cells. RNA was extracted 72 h post transfection (h.p.t.), followed by RT-PCR and sequence analysis.

Figure 3. Replication and translation of CHIKV AUD mutants in mammalian cells at 28°C or 37°C. C2C12 were transfected with WT and mutant CHIKV-SGR-D-Luc RNAs and cultured at 28°C or 37°C. Cells were harvested at indicated time points. (**A**) FF-Luc activities of WT and mutants were measured and normalized to their respective 4 h values, which thus represent fold-change compared to the 4 h values. Significant differences denoted by ** (P<0.01), *** (P<0.001) **** (P<0.0001), compared to WT are only shown for the 12 h time point for clarity. Data are displayed as the means ±S.E. of three experimental replicates. (**B**) Protein expression of nsP1 for the WT and mutant CHIKV-SGR-D-Luc at 28°C or 37°C. Cells were lysed at 24 h.p.t., 10 µg of each sample was loaded and analysed by western blot. Actin was also detected by western blot as a loading control. (**C**) Quantification of CHIKV positive and negative strand RNA from C2C12 cells transfected with CHIKV-SGR-D-luc. Transfected C2C12 cells from (**A**) were lysed with TRIzol solution, and total RNA was purified by phenol-chloroform extraction. cDNAs of CHIKV positive or negative strand RNA were synthesized as described before [54]. Quantitative PCR was performed at 95°C for 2 min., followed by 40 cycles of 95°C for 5 s and 60°C for 30 s.

Figure 4. Replication of CHIKV SGRs, Bunyamwera (BUNV) mini-genome and Zika SGR at 28°C or 37°C. (**A**) Schematic of CHIKV SGRs. CHIKV SGR-nsP3-mCh-FF-Luc was constructed in which the R-Luc reporter in CHIKV SGR-D-luc (Fig 1A) was replaced with mCherry. CHIKV SGR-FF-Luc was constructed by deleting R-Luc and thus expressing WT unfused nsP3. **(B)** C2C12 cells were transfected with the three CHIKV SGRs and incubated at 28°C or 37°C. Cells were harvested at indicated time points. FF-Luc activities of WT and mutants were measured and normalized to their respective 4 h values and thus represent fold-change compared to those 4 h values (GAA: nsP4 polymerase inactive mutant). Significant differences denoted by ns (P>0.05), * (P<0.05), ** (P<0.01), *** (P<0.001) **** (P<0.0001), are only shown for the 12 h time point for clarity. Data are displayed as the means ±S.E. of three experimental replicates. Replication of BUNV mini-genome (**C**) and Zika virus SGR **(D)** at 28°C or 37°C. Cells were collected at indicated time points and R-Luc or nano-luciferase (nano-luc) activities were measured and normalized to their respective 4 h values.

Figure 5. Phenotype of WT and AUD mutants in the context of ICRES-CHIKV at 28°C or 37°C. (**A**) Phenotype of WT and AUD mutants in ICRES-CHIKV production at 28°C or 37°C. C2C12 cells were transfected with WT and mutant ICRES-CHIKV RNA and incubated at 28°C or 37°C. Supernatants were collected 48 h post infection (h.p.i.) from both temperatures and titrated at 37°C by plaque assay. (**B**) One step growth curve of ICRES-CHIKV in C2C12 cells at 28°C or 37°C. C2C12 cells were infected with ICRES-CHIKV at MOI 0.1 and incubated at 37°C or 28°C respectively. Cell supernatants were collected at indicated time points and virus titers were determined by plaque assay. (**C**) CHIKV RNA quantification from infected C2C12 cells. C2C12 cells collected at indicated

time points were lysed by TRIzol solution, and total RNA were purified by phenol-chloroform extraction. cDNAs of CHIKV positive or negative strand RNA were synthesized as described before [58]. Quantitative PCR for different samples were performed at 95°C for 2 min; followed by 40 cycles of 95°C for 5 s and 60°C for 30 s.

Figure 6. Temperature shift assay of WT SGR-D-Luc. (**A**) Schematic of temperature shift assay. Transfected cells were incubated at either 28°C or 37°C prior to a temperature shift from 12-24 h.p.t. (28°C to 37°C (designated 24 h S*), or 37°C to 28°C (designated 24 h S#). Controls maintained the same temperature from 0-24 h.p.t. (**B**) Replication of WT CHIKV-SGR-D-Luc at 28°C or 37°C. WT CHIKV-SGR-D-Luc RNA was transfected into C2C12 cells and incubated at 28°C or 37°C according to the schematic in **(A)**. FF-Luc activities were measured and normalized to their respective 4 h values. Significant differences denoted by ** (P<0.01), **** (P<0.0001), compared to replication at 12 h.p.t. Data are displayed as the means ±S.E. of three experimental replicates. Cell numbers were enumerated (**C**) and cell metabolic activity **(D)** determined by MTT assay at 28°C or 37°C. **(E)** Protein expression of nsP1 and P-eIF2α at 28°C or 37°C. Cells were lysed at 24 h.p.t. and 10 µg of each sample was analysed by western blot. Total eIF2α and Actin were also detected by western blot as loading controls.

Figure 7. Formation of cytoplasmic nsP3/dsRNA positive foci at 28°C or 37°C. (**A**) C2C12 cells were transfected with WT CHIKV-SGR-nsP3-mCh-FF-Luc and incubated at 28°C or 37°C respectively. Cells were then fixed with 4% paraformaldehyde and stained with antibodies to G3BP (Green) or dsRNA (gray). nsP3-mCherry was expressed as a fused protein (Red). Scale bar 10 µm. (**B**) Quantification of the overall dsRNA, nsP3-mCherry and G3BP expression at 28°C or 37°C. Protein expression levels were

determined for 10 cells and calculated by Fiji ImageJ. Significant differences denoted by ns (P>0.05), * (P<0.05), *** (P<0.001), **** (P<0.0001), compared to values at 37°C.

Figure 8. Co-localisation of G3BP with nsP3 and dsRNA at 28°C or 37°C. (**A**) Detection of dsRNA, nsP3 and G3BP in WT CHIV-SGR-nsP3-mCh-FF-Luc transfected C2C12 cells. Immunofluorescence assay were performed as before. Co-localisation of dsRNA, nsP3 and G3BP were shown. All image analysis and processing was performed using Fiji software. Fluorescence plot profile of nsP3, dsRNA and G3BP signal intensities along the indicated white line is shown. (**B**) Quantitative analysis of the colocalization between dsRNA, nsP3 and G3BP signals. Pearson's correlation coefficient between dsRNA and G3BP, nsP3 and G3BP, dsRNA and nsP3 were determined for 10 cells and calculated by Fiji ImageJ. Significant differences denoted by ns (P>0.05), **** (P<0.0001), compared to values at 37°C.

Figure 9. Co-localisation of eIF4G or TIA-1 with nsP3/dsRNA positive cytoplasmic foci at 28°C and 37°C. Detection of dsRNA, nsP3 and eIF4G (**A**) or TIA-1 (**B**) in WT CHIKV-SGR-nsP3-mCh-FF-Luc transfected C2C12 cells. Immunofluorescence assays were performed as before. Co-localisation of dsRNA, nsP3 and eIF4G or TIA-1 are shown. All image analysis and processing was performed using Fiji software. Fluorescence plot profile of nsP3, dsRNA and eIF4G or TIA-1 signal intensities along the white line is shown. (**C**) Quantitative analysis of the colocalization between dsRNA, nsP3 and eIF4G or TIA-1 signals. Pearson's correlation coefficients were determined for 10 cells and calculated by Fiji ImageJ. Significant differences denoted by ns (P>0.05), **** (P<0.0001), compared to values at 37°C.

A

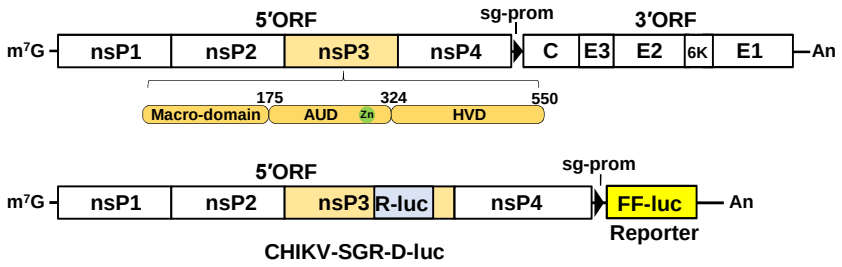
5′ORF
sg-prom
3′ORF
m7G
nsP1
nsP2
nsP3
nsP4
C
E3
E2
6K
E1
An
175
324
550
Macro-domain
AUD
Zn
HVD
5′ORF
sg-prom
m7G
nsP1
nsP2
nsP3
R-luc
nsP4
FF-luc
An
Reporter
CHIKV-SGR-D-luc

B

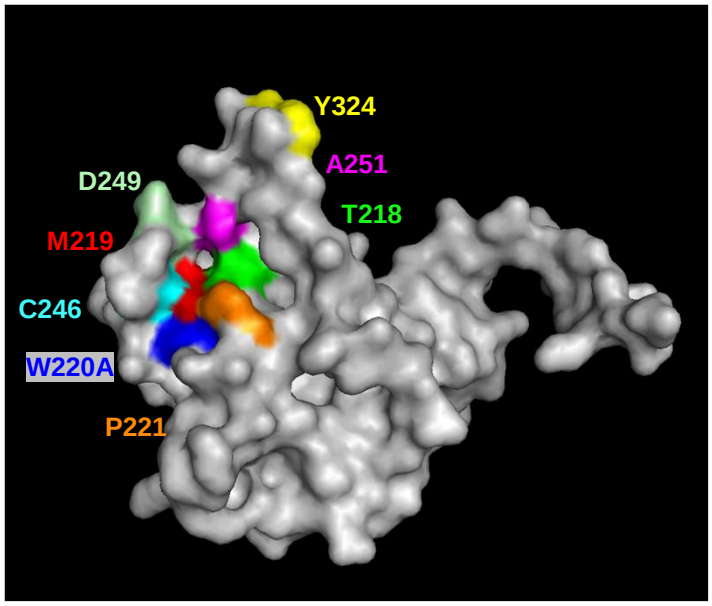
Y324
A251
D249
T218
M219
C246
W220A
P221

Figure 1

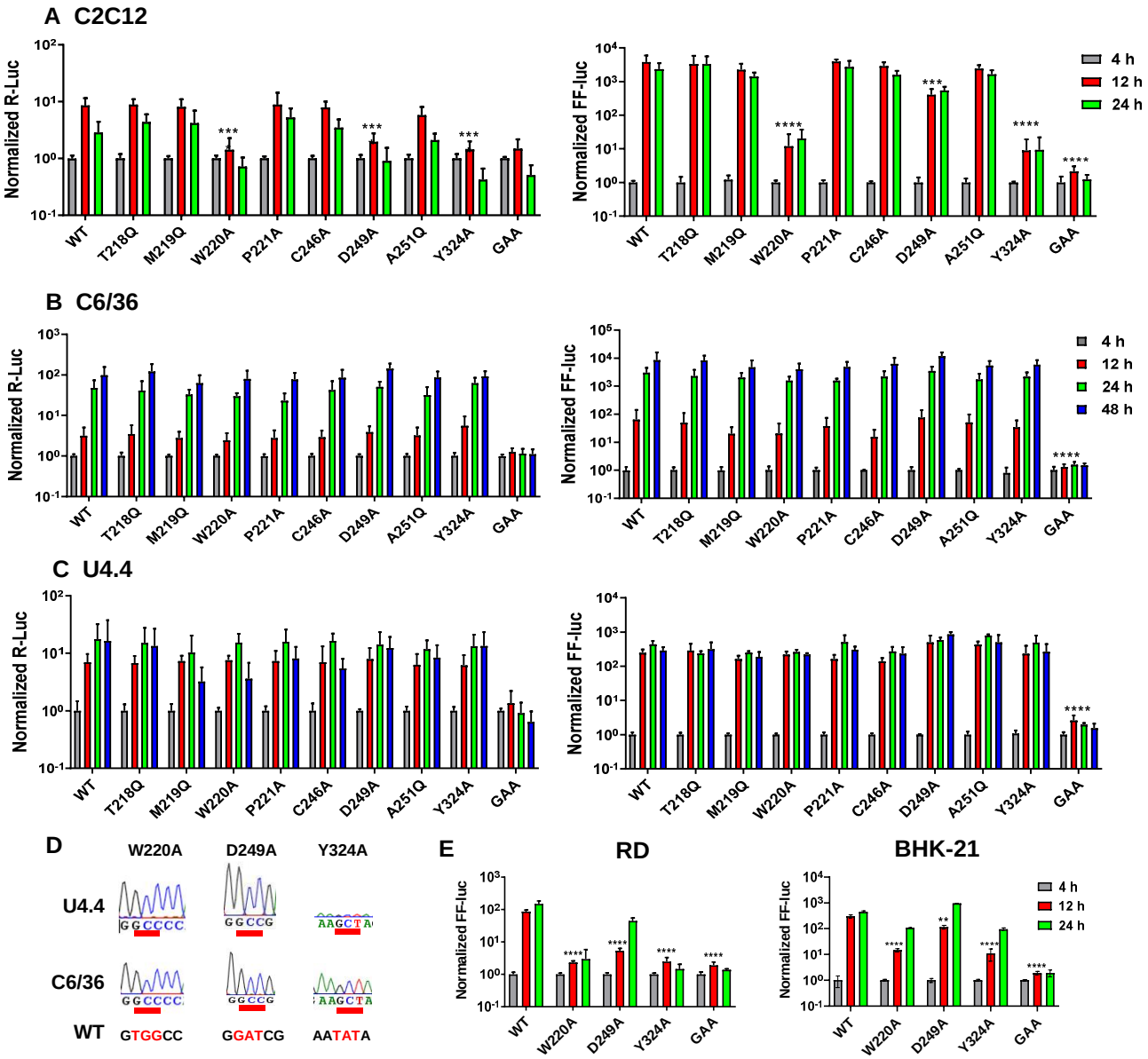
A C2C12
Normalized R-Luc
Normalized FF-luc
4 h
12 h
24 h
WT
T218Q
M219Q
W220A
P221A
C246A
D249A
A251Q
Y324A
GAA
B C6/36
48 h
C U4.4
D
W220A
D249A
Y324A
U4.4
C6/36
WT
GTGGCC
GGATCG
AATATA
E
RD
BHK-21

Figure 2

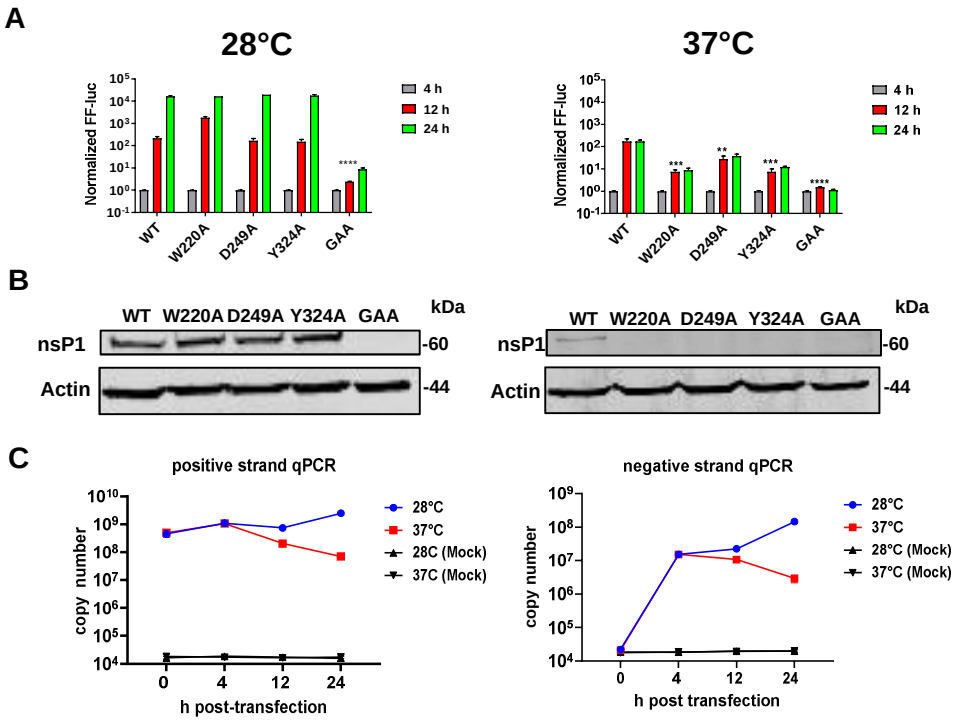
A
28°C
37°C
Normalized FF-luc
4 h
12 h
24 h
WT
W220A
D249A
Y324A
GAA
B
kDa
nsP1
Actin
-60
-44
C
positive strand qPCR
negative strand qPCR
copy number
28°C
37°C
28C (Mock)
37C (Mock)
28°C (Mock)
37°C (Mock)
h post-transfection
h post transfection

Figure 3

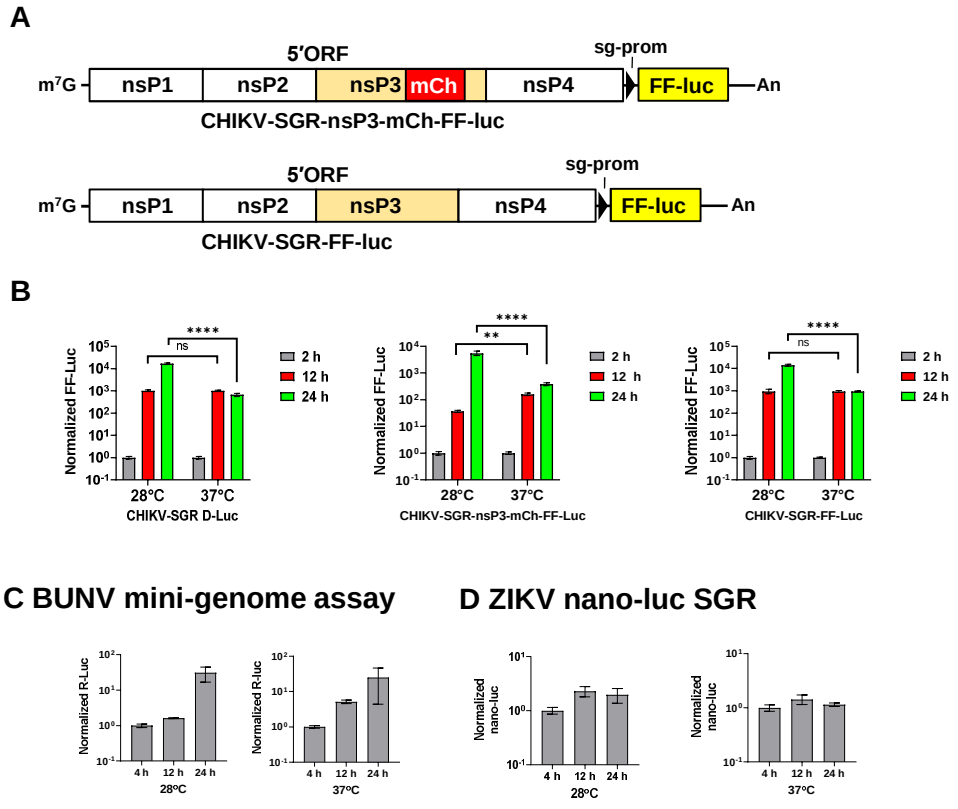
A
5′ORF
sg-prom
m7G
nsP1
nsP2
nsP3
mCh
nsP4
FF-luc
An
CHIKV-SGR-nsP3-mCh-FF-luc
5′ORF
sg-prom
m7G
nsP1
nsP2
nsP3
nsP4
FF-luc
An
CHIKV-SGR-FF-luc
B
Normalized FF-Luc
****
ns
2 h
12 h
24 h
28°C
37°C
CHIKV-SGR D-Luc
Normalized FF-Luc
****
**
2 h
12 h
24 h
28°C
37°C
CHIKV-SGR-nsP3-mCh-FF-Luc
Normalized FF-Luc
****
ns
2 h
12 h
24 h
28°C
37°C
CHIKV-SGR-FF-Luc
C BUNV mini-genome assay
D ZIKV nano-luc SGR
Normalized R-Luc
4 h
12 h
24 h
28°C
Normalized R-luc
4 h
12 h
24 h
37°C
Normalized nano-luc
4 h
12 h
24 h
28°C
Normalized nano-luc
4 h
12 h
24 h
37°C

Figure 4

A ICRES-CHIKV titre

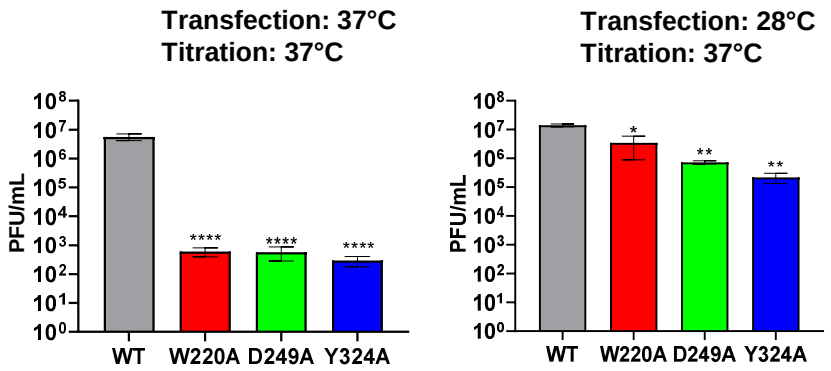

B One step growth curve of ICRES-CHIKV

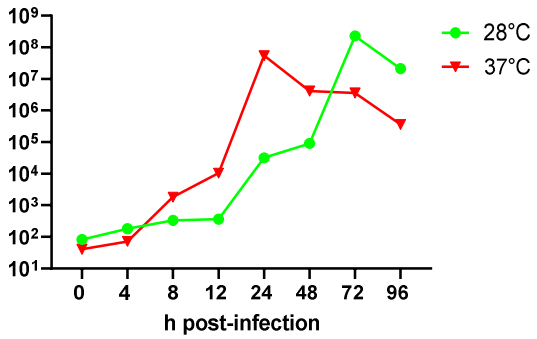

C ICRES-CHIKV RNA quantification

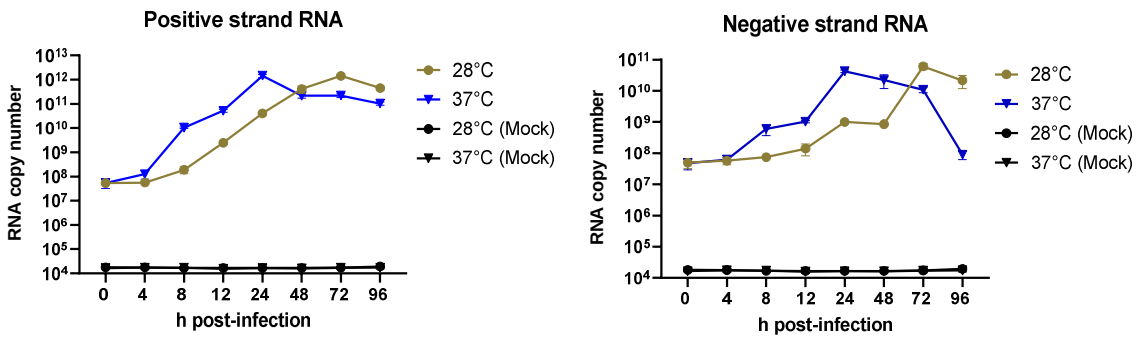

Figure 5

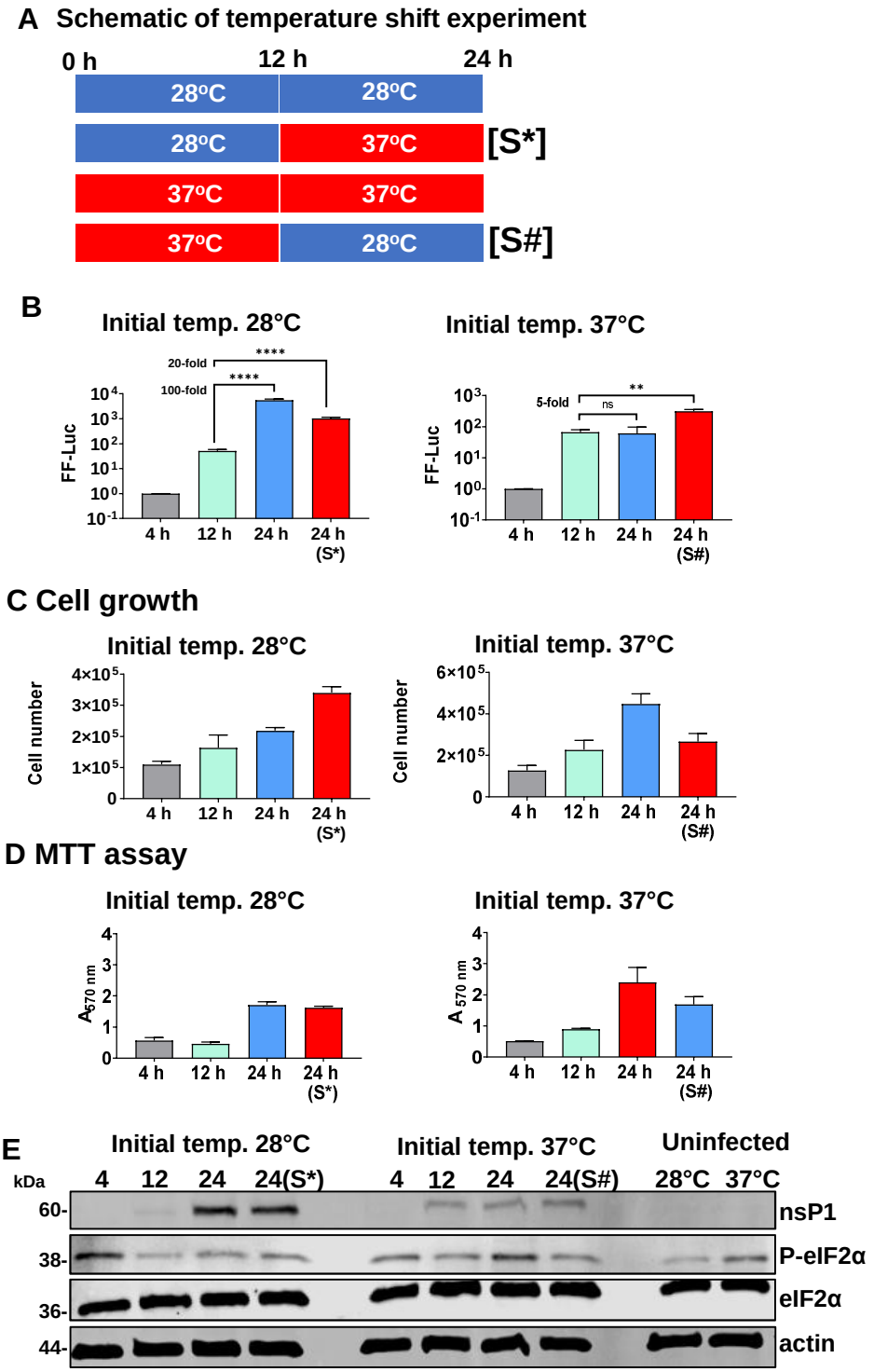
A Schematic of temperature shift experiment
0 h
12 h
24 h
28ºC
28ºC
28ºC
37ºC
[S*]
37ºC
37ºC
37ºC
28ºC
[S#]
B
Initial temp. 28°C
Initial temp. 37°C
FF-Luc
20-fold
100-fold
5-fold
ns
4 h
12 h
24 h
24 h (S*)
24 h (S#)
C Cell growth
Cell number
D MTT assay
A570 nm
E
kDa
4
12
24
24(S*)
24(S#)
28°C
37°C
Uninfected
60-
38-
36-
44-
nsP1
P-eIF2α
eIF2α
actin

Figure 6

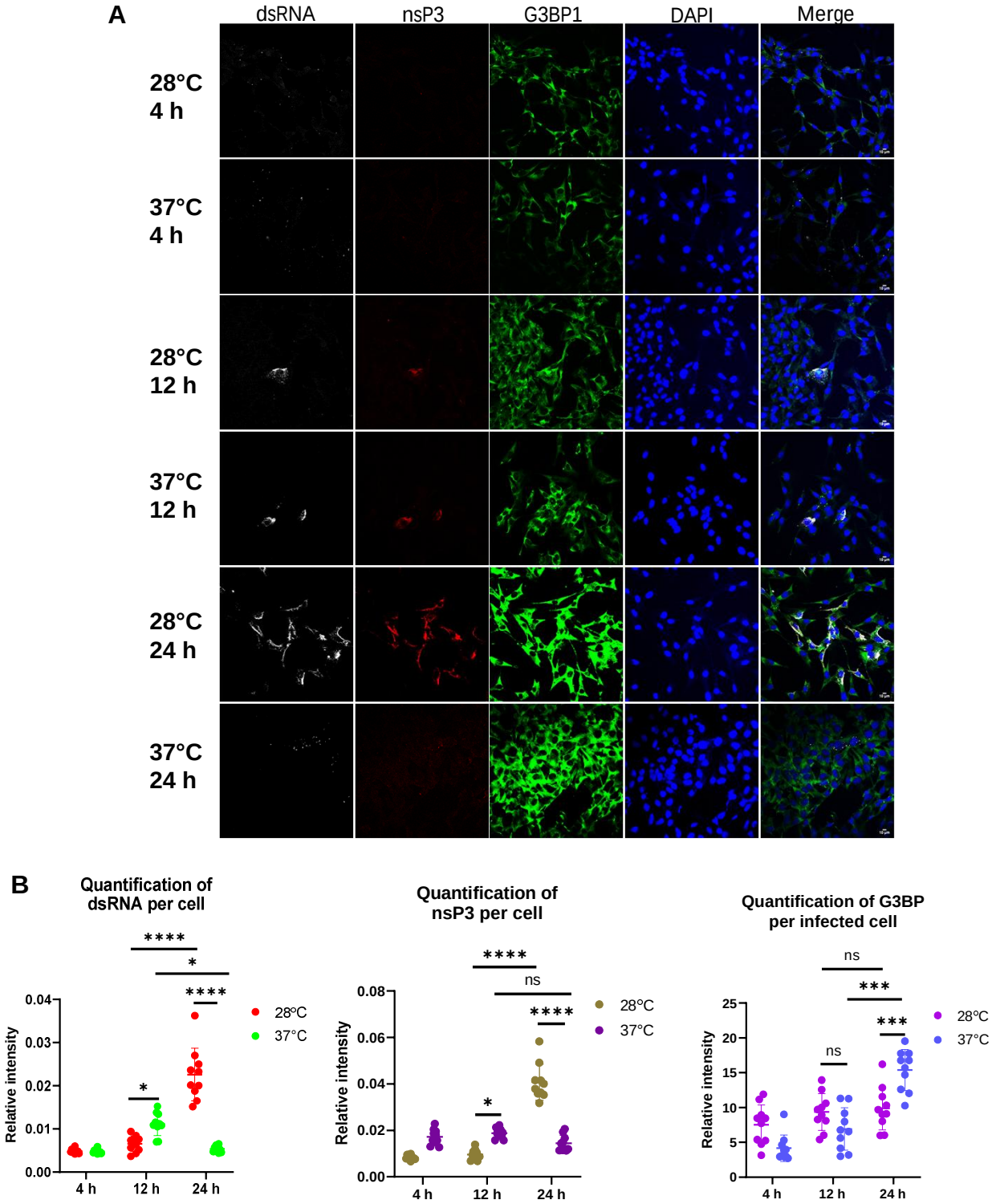
A
dsRNA
nsP3
G3BP1
DAPI
Merge
28°C 4 h
37°C 4 h
28°C 12 h
37°C 12 h
28°C 24 h
37°C 24 h
B
Quantification of dsRNA per cell
Relative intensity
0.04
0.03
0.02
0.01
0.00
4 h
12 h
24 h
****
*
28°C
37°C
Quantification of nsP3 per cell
0.08
0.06
0.04
0.02
0.00
ns
Quantification of G3BP per infected cell
25
20
15
10
5
0
***

Figure 7

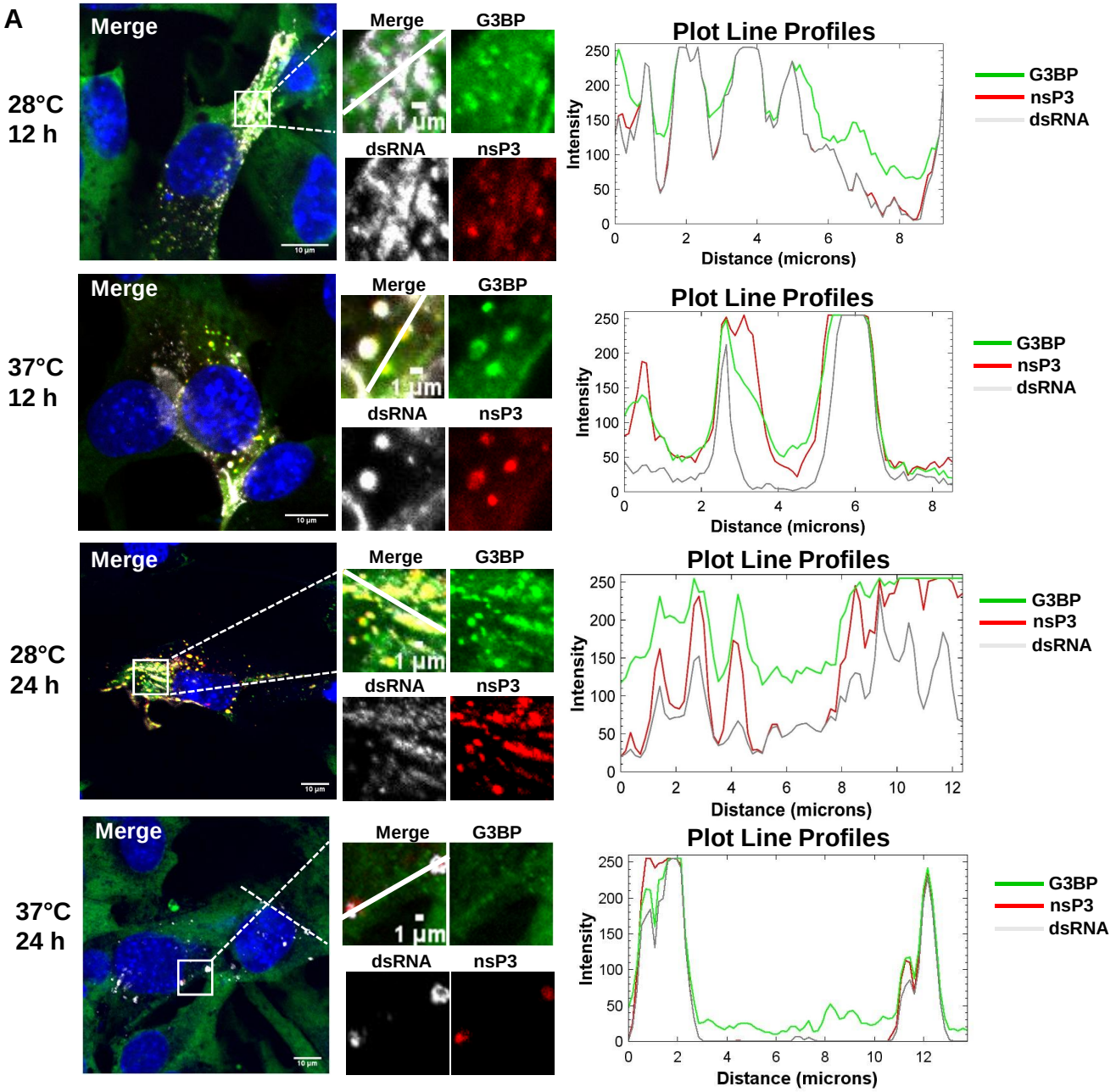
A
28°C
12 h
37°C
12 h
28°C
24 h
37°C
24 h
Merge
G3BP
dsRNA
nsP3
1 µm
10 µm
Plot Line Profiles
Intensity
Distance (microns)
G3BP
nsP3
dsRNA

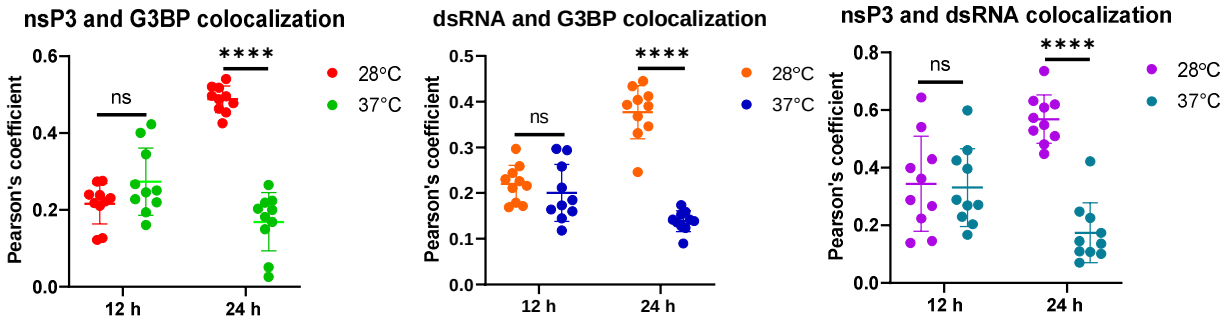
B
nsP3 and G3BP colocalization
dsRNA and G3BP colocalization
nsP3 and dsRNA colocalization
Pearson's coefficient
ns
****
28°C
37°C
12 h
24 h

Figure 8

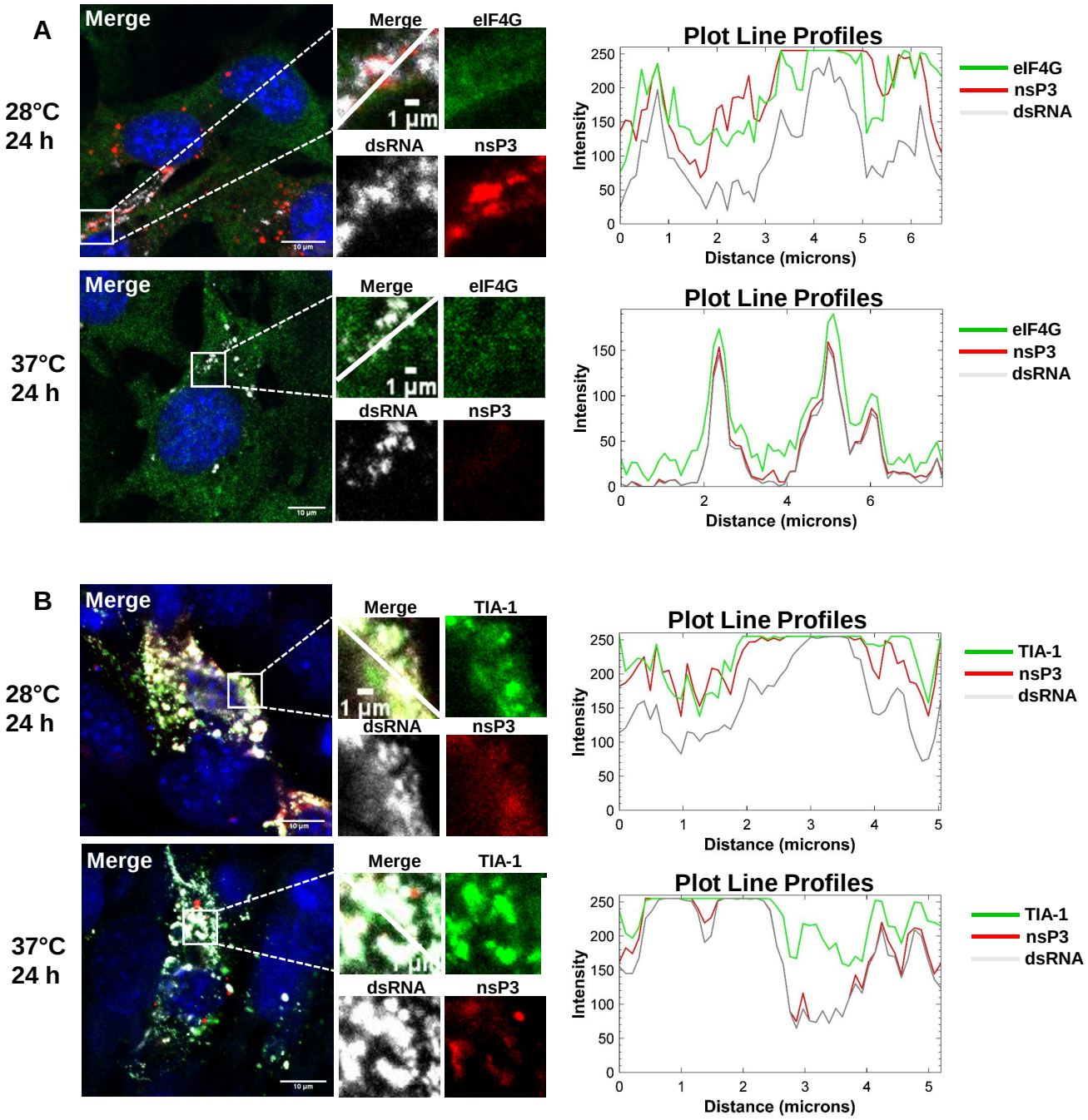
A
28°C
24 h
Merge
Merge
eIF4G
1 µm
dsRNA
nsP3
Plot Line Profiles
Intensity
Distance (microns)
eIF4G
nsP3
dsRNA
37°C
24 h
B
TIA-1
C
nsP3 and TIA-1/eIF4G colocalization
dsRNA and TIA-1/eIF4G colocalization
nsP3 and dsRNA colocalization
Pearson's coefficient
28°C
37°C
TIA-1
eIF4G
24 h
ns

Figure 9